Cluster Compounds

DOI: 10.1002/ange.201200072

The Importance of Being Exchanged: $[Gd^{III}_4M^{II}_8(OH)_8(L)_8(O_2CR)_8]^{4+}$ Clusters for Magnetic Refrigeration**

Thomas N. Hooper, Jürgen Schnack, Stergios Piligkos, Marco Evangelisti,* and Euan K. Brechin**

One of the most promising applications for molecules built from paramagnetic metal ions is low-temperature magnetic refrigeration.[1] Indeed, recent studies have suggested that molecular coolers can outperform any conventionally employed solid-state refrigerant material by orders of magnitude.[2] In order to do so, molecules must possess a combination of a large spin ground state (S), with negligible anisotropy ($D_{cluster} = 0$), weak magnetic exchange between the constituent metal ions, and a relatively large metal:non-metal mass ratio (that is, a large magnetic density).[1b] These molecular prerequisites suggest the use of lanthanide ions and, in particular, the f^7 ion Gd^{3+} in the construction of homo- and heterometallic (Gd-3d) clusters, and a sensible starting point is the synthesis of Gd^{III}–Cu^{II} clusters, as previous studies have shown this combination favors ferromagnetic exchange.[3]

Herein we introduce a rather remarkable new family of compounds of general formula $[Ln^{III}_4M^{II}_8(OH)_8(L)_8(O_2CR)_8](X)_4$ in which almost all the constituent parts, namely the lanthanide ions Ln^{3+}, the transition-metal ions M^{2+}, the bridging ligand L, the carboxylates, and the counterions X can be exchanged. In each case, the structure remains essentially the same and this allows for a thorough understanding of the individual contributions to the magnetocaloric effect (MCE). Herein we describe the three family members $[Gd^{III}_4M^{II}_8(OH)_8(L)_8(O_2CR)_8](ClO_4)_4$ (M = Zn, R = $CHMe_2$, **1**; M = Cu, R = $CHMe_2$, **2**; M = Ni, R = CH_2Me, **3**; LH = 2-(hydroxymethyl)pyridine) and show how the identity of the transition metal and the sign of the magnetic exchange are vital components to consider when designing molecular coolers.

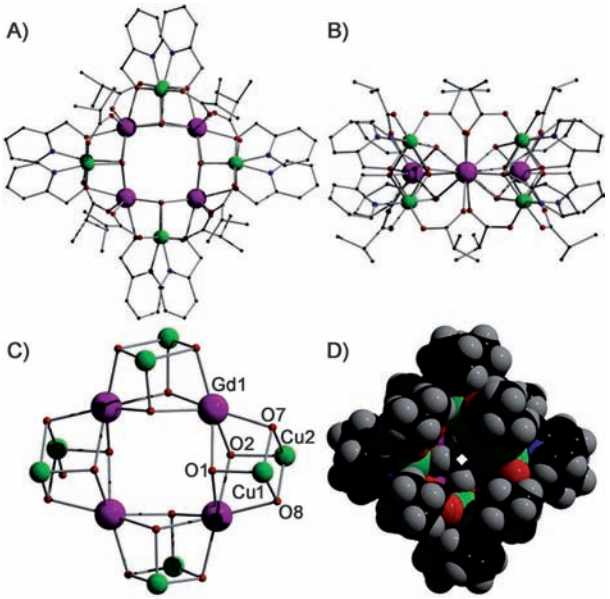

Figure 1. The molecular structure of the cation of complex **2** viewed perpendicular (A) and parallel (B) to the $\{Gd_4\}$ plane. Gd purple, Cu green, O red, N blue, C black. Hydrogen atoms and the ClO_4^- anions are omitted for clarity. C) The metal–oxygen core, indicating the corner-sharing $\{Gd_2Cu_2O_4\}$ cubanes; Cu-O-Cu = 95.64–96.56°, Cu-O-Gd = 95.26–101.87°, Gd-O-Gd = 110.90–111.88°. D) Space-filling representation of the cation of **2**.

For the sake of brevity, we provide a generic structure description, highlighting any differences. The core of the molecule (Figure 1 shows complex **2**) consists of a square (or wheel) of four corner-sharing $\{Gd^{III}_2M^{II}_2O_4\}^{6+}$ cubanes. The shared corners are the Gd ions, which thus themselves form an inner $\{Gd^{III}_4\}$ square, each edge of which is occupied by two μ_3-OH^- ions that further bridge to an M^{II} ion. The μ_3-L^- ions chelate the M^{2+} ions and use their O-arm to further bridge to the second M^{2+} ion in the same cubane and to one Gd ion. There are two carboxylates per cubane, each μ-bridging across a $M^{2+}\cdots$Gd square face, alternately above and below the plane of the $\{Gd^{III}_4\}$ square.

A comparison of the structure of **1** (Supporting Information, Figure S1) with **2** shows them to be very similar. The

[*] Dr. T. N. Hooper, Prof. E. K. Brechin
EaStCHEM School of Chemistry, The University of Edinburgh
West Mains Road, Edinburgh, EH93JJ (UK)
E-mail: ebrechin@staffmail.ed.ac.uk
Prof. J. Schnack
Universität Bielefeld, Fakultät für Physik
Postfach 100131, 33501 Bielefeld (Germany)
Dr. S. Piligkos
Department of Chemistry, University of Copenhagen
Universitetsparken 5, 2100 Copenhagen (Denmark)
E-mail: piligkos@kiku.dk
Dr. M. Evangelisti
Instituto de Ciencia de Materiales de Aragón, CSIC-Universidad de Zaragoza, Departamento de Física de la Materia Condensada
50009 Zaragoza (Spain)
E-mail: evange@unizar.es

[**] E.K.B. wishes to thank the EPSRC for funding. M.E. acknowledges contracts MAT2009-13977-C03 and CSD2007-00010. S.P. thanks the Danish Natural Science Research Council for a Sapere Aude Fellowship (10-081659). Computing time at the Leibniz Computing Centre in Garching is gratefully acknowledged. LH = 2-(hydroxymethyl)pyridine, R = CH_2Me, $CHMe_2$, M = Zn, Cu, Ni.

Supporting information for this article is available on the WWW under http://dx.doi.org/10.1002/anie.201200072.

central $\{Gd_4(OH)_8\}$ square motif is almost identical, with the copper structure forming a perfect square (as enforced by crystallographic symmetry), whilst the zinc structure deviates only very slightly, with Gd-Gd-Gd angles of 90.87 and 89.17°. In **2**, the Cu^{II} ions are in a square-based pyramidal geometry with the Jahn–Teller axes being the apex of the pyramid. In **1**, the L^- ligands have rotated approximately 45° out of the plane of the face of the cube, affording a more trigonal bipyramidal geometry at the Zn center, reflecting the lack of electronic stabilization afforded to a d^{10} ion. Comparison of **1** and **2** with **3** (Supporting Information, Figure S2) however does show some significant differences. The bond lengths and angles within the cubes of the $\{Gd_4Ni_8\}$ and $\{Gd_4Zn_8\}$ structures are similar but the $\{Gd_4(OH)_8\}$ motif in **3** has distorted to a more rhombus-like shape, with Gd-Gd-Gd angles of 95.66 and 84.34°. Each Ni^{II} center is octahedral with six methanol molecules bonding to one nickel center each, with a change in the coordination of the carboxylates filling the coordination spheres of the remaining two nickel centers. The carboxylate ligands have lost the regular alternating pattern seen in **1** and **2**: six remain in *syn*, *syn*, μ-coordination mode, bridging across a Gd···Ni square face, but two are now μ_3-bridging (Ni···Gd···Ni) in a *syn*, *syn-anti* fashion across two Gd···Ni square faces.

A search of the CCDC database reveals that there are only two other $[Ln^{III}_4M^{II}_8]$ complexes reported, $[Gd^{III}_4Co^{II}_8(OH)_4(NO_3)_4(O_3PtBu)_8(O_2CtBu)_{16}]$ and $[Gd^{III}_4Co^{II}_8(O_3PtBu)_6(O_2CtBu)_{16}]$.[4] Other molecules with closely related structures are the complex $[Dy^{III}_3Cu^{II}_6L_6(OH)_6(H_2O)_{10}]Cl_2{\cdot}ClO_4$ (LH_2 = 1,1,1-trifluoro-7-hydroxy-4-methyl-5-azahept-3-en-2-one), the structure of which describes a triangle (or wheel) of three $\{Dy^{III}_2Cu^{II}_2O_4\}$ cubanes,[5] and the square-in-a-square complexes $[Mn^{III}_4Ln^{III}_4(OH)_4(C[4])_4(NO_3)_2(H_2O)_6](OH)_2$ (C[4] = calix-[4]arene) and $[Mn^{III}_4Ln^{III}_4(\mu_3\text{-}OH)_4(N_3)_4(O_2CtBu)_8(t\text{-bdea})_4]$ (*t*-bdea = *t*-butyldiethanolamine) containing four corner-sharing $\{Ln^{III}_2Mn^{III}O_4\}$ partial cubanes.[6]

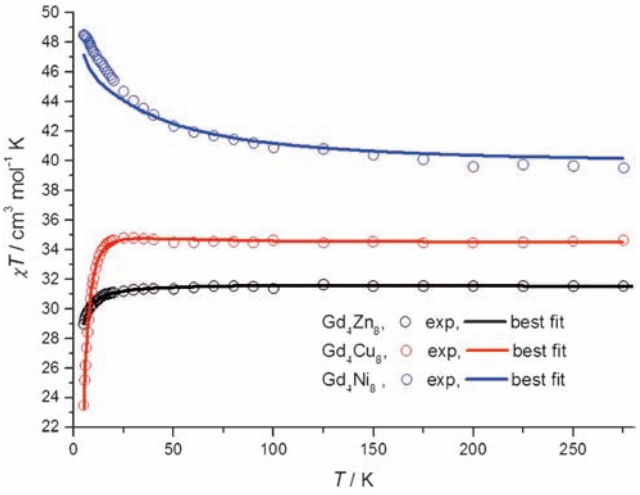

Figure 2. $\chi_M T$ products of **1**, **2**, and **3** in a magnetic field of 0.1 T in the temperature range 5 to 275 K. The experimental data have been interpreted as explained in the text.

The dc magnetic susceptibilities of **1**–**3** were measured in an applied field B_0 of 0.1 T over the 5 to 275 K temperature range, and are shown in Figure 2 in the form of $\chi_M T$ products. At 275 K, the obtained $\chi_M T$ values of 31.5, 34.5, and 39.5 $cm^3 K mol^{-1}$ are exactly those expected for spin-only contributions to the magnetism of $[Gd^{III}_4M^{II}_8]$ (M = Zn, Cu, and Ni, respectively) with $g = 2.00$. The temperature dependence of the $\chi_M T$ product of **1** indicates the absence of sizeable exchange interactions between the Gd^{III} ions. The spin-Hamiltonian matrix of **1** is a square matrix of dimension 4096 and can be diagonalized by standard full-matrix approaches. The $\chi_M T$ data of **1** can be fitted to a simple isotropic model containing a unique magnetic exchange-interaction parameter, describing a $\{Gd^{III}_4\}$ square to afford $J_{Gd\text{-}Gd} = 0.02\ cm^{-1}$. The temperature dependence of the $\chi_M T$ products of **2** and **3** suggest the presence of ferri- and ferromagnetic exchange interactions, respectively. The data can be successfully fitted with the isotropic model of Equation (1) that contains three

$$\begin{aligned}\hat{H} &= g\mu_B B_0 \sum_i \hat{S}_i + \\ &\sum \left\{ J_{GdGd}\left(\hat{S}_1\hat{S}_2 + \hat{S}_2\hat{S}_3 + \hat{S}_3\hat{S}_4 + \hat{S}_4\hat{S}_1\right)\right\} + \\ &\sum \left\{ J_{MM}\left(\hat{S}_5\hat{S}_6 + \hat{S}_7\hat{S}_8 + \hat{S}_9\hat{S}_{10} + \hat{S}_{11}\hat{S}_{12}\right)\right\} + \\ &\sum \left\{ J_{GdM}\left[\begin{array}{l}\hat{S}_1\left(\hat{S}_5 + \hat{S}_6 + \hat{S}_{11} + \hat{S}_{12}\right) + \hat{S}_2\left(\hat{S}_5 + \hat{S}_6 + \hat{S}_7 + \hat{S}_8\right) + \\ \hat{S}_3\left(\hat{S}_7 + \hat{S}_8 + \hat{S}_9 + \hat{S}_{10}\right) + \hat{S}_4\left(\hat{S}_9 + \hat{S}_{10} + \hat{S}_{11} + \hat{S}_{12}\right)\end{array}\right]\right\}\end{aligned} \quad (1)$$

distinct magnetic exchange-interaction parameters, where $\hat{S}$ is a single-ion spin operator, the index i runs through all twelve centers of **2** and **3** (Gd^{III} ions correspond to indices 1 to 4), $g = 2$ is the isotropic g factor, and μ_B is the Bohr magneton. The spin-Hamiltonian matrix of **2** is of dimension 1 048 576 and cannot be diagonalized in the same way as for **1**. For **2**, we used self-written software (ITO-MAGFIT[7]) that makes use of irreducible tensor operator algebra[8] to block-diagonalize the spin-Hamiltonian. ITO-MAGFIT is a magnetization fitting program using the Levenberg–Marquardt algorithm.[9] The best-fit exchange parameters determined in this way for **2** are: $J_{CuCu} = 11.84\ cm^{-1}$, $J_{GdCu} = -1.38\ cm^{-1}$, and $J_{GdGd} = 0.20\ cm^{-1}$.

The spin-Hamiltonian matrix of **3** is of dimension 26 873 856 and cannot be treated by complete matrix diagonalization. Magnetic observables of such spin systems can nevertheless be accurately determined with the finite-temperature Lanczos method.[10] However, because the numerical effort is still enormous, the program makes use of open MP parallelization[11] and has been executed on 40 cores of the SuperMUC Supercomputer at LRZ Garching/Germany as well as on a supercomputer at Bielefeld University.

Thus, the magnetism data of **3** have been interpreted by successive simulations and not by a numerical fitting routine as for **1** and **2**. The obtained exchange parameters are: $J_{NiNi} = -24.0\ cm^{-1}$, $J_{GdNi} = -0.34\ cm^{-1}$, and $J_{GdGd} = 0.20\ cm^{-1}$. The $\chi_M T$ product of **3** is very sensitive to the magnitude of the J_{NiNi} exchange interaction. In fact, the experimental data could also be reproduced by a parameter set involving an anti-

ferromagnetic Ni–Ni exchange interaction: $J_{NiNi} = 6.0\ cm^{-1}$, $J_{GdNi} = -1.32\ cm^{-1}$, and $J_{GdGd} = 0.20\ cm^{-1}$. This uncertainty could not be resolved, as simplifying assumptions, such as $g = 2.00$, had to be made to make the numerical treatment feasible at all. Nevertheless, as the Ni-O-Ni angle is approximately 96°, the exchange is most likely of ferromagnetic nature, as found in all other Ni^{2+} compounds.[12]

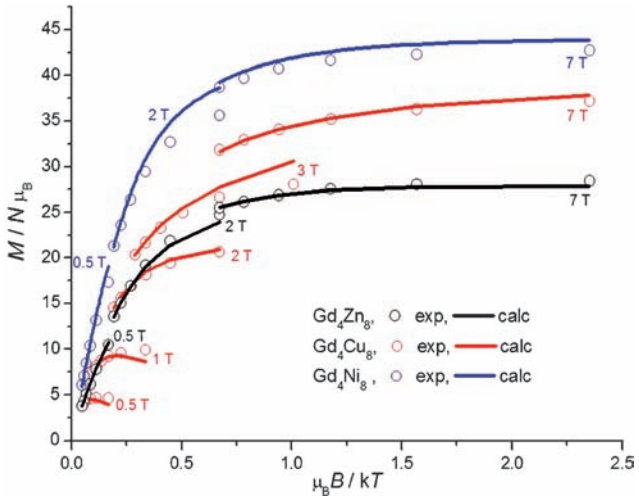

Figure 3. Reduced magnetization data of **1**, **2**, and **3** in the temperature range 2 to 7 K and the field range 0.5 to 7 T. The experimental data have been interpreted as explained in the text.

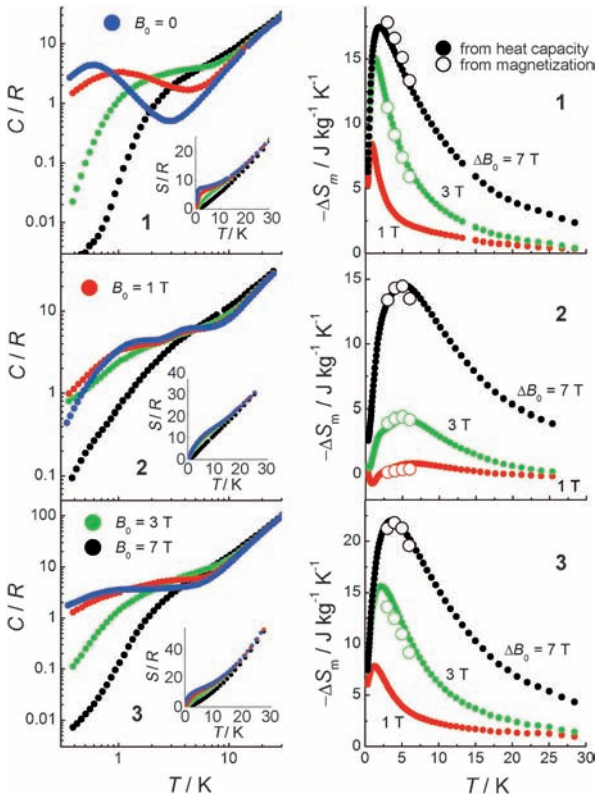

Figure 4. Left: From top to bottom, temperature dependencies of the heat capacities and entropies (insets) of **1**, **2**, and **3**, respectively, for selected applied magnetic fields, as labeled. Right: From top to bottom, temperature dependencies of the magnetic entropy changes, as obtained from *C* (filled dots) and *M* data (empty dots), for **1**, **2**, and **3**, respectively, for selected applied magnetic field changes, as labeled.

Magnetization measurements (Figure 3) show saturation values of approximately 28, 38, and 44 $N\mu_B$ for **1**–**3**, respectively, suggestive of $S = 22$ for **3**, and field-induced $S = 14$ and $S = 18$ ground states for **1** and **2**. The reduced magnetization data can be reproduced by single-point calculations using the parameters determined from the interpretation of the $\chi_M T$ products of **1**–**3** (Figure 3).

The experimental heat capacity *C*, normalized to the gas constant *R*, of the investigated complexes is shown in the left panels of Figure 4 as a function of temperature for selected applied magnetic fields B_0. As expected, high-temperature *C* is dominated by nonmagnetic contributions arising from thermal vibrations of the lattice. At low temperatures, *C* is dominated by an applied-field sensitive contribution, which shifts to higher temperatures by increasing B_0. No phase transition is detected down to about 0.3 K, indicating that the involved magnetic interactions are weak. From the experimental heat capacity, the temperature dependence of the entropy is obtained by integrating $\int C/T\mathrm{d}T$, leading to the entropy curves depicted in the insets of Figure 4 for the corresponding applied fields. In agreement with the magnetization data, Figure 4 shows that the magnetic contributions to the heat capacity extend towards much higher temperatures in the cases of **2** and **3**, thus proving the presence of (relatively) stronger exchange coupling for these two complexes.

Indeed for **1**, the magnetic contribution to the zero-field *C* takes place at extremely low temperatures, giving rise to an entropy that increases sharply, reaching an approximate value of $7R$. The $2\ K < T < 6\ K$ temperature range is characterized by a slow increase of the zero-field entropy, passing from $7.2R$ to $8R$. Above roughly 6 K, the zero-field entropy starts to steadily increase because of the lattice contribution. The 7–8*R* plateau can be understood by assuming that all the $Gd^{3+}\cdots Gd^{3+}$ interactions are gradually decoupling. Therefore, we expect the entropy to approach the maximum value for non-interacting single-ion spins, that is, $4R\ln(2S_{Gd}+1) = 8.3R$, where $S_{Gd} = 7/2$, which is in excellent agreement with the experimental data.

The evaluation of the MCE includes the calculation of the magnetic entropy change ΔS_m for selected applied field changes ΔB_0, from the measured heat capacity and magnetization. As for the former, ΔS_m can be obtained from the temperature and field dependencies of the entropy. The results are summarized in the right panels of Figure 4, together with the estimates obtained by applying the Maxwell relation, $\Delta S_m(T) = \int[\partial M/\partial T]\mathrm{d}B_0$, to the magnetization *M* data of Figure 3. Good agreement is observed between the two procedures. For $\Delta B_0 = 7$ T, we observe the largest $-\Delta S_m$ for **3**, which reaches $22.0\ J\,kg^{-1}K^{-1}$ at $T = 3.6$ K. This maximum decreases down to $18.0\ J\,kg^{-1}K^{-1}$ at $T = 2.0$ K for **1**, which is close to the full available entropy content of $20.8\ J\,kg^{-1}K^{-1}$. For **2**, the maximum $-\Delta S_m$ decreases further, reaching $14.6\ J\,kg^{-1}K^{-1}$, although at the relatively higher temperature

$T = 5.6$ K. The fact that the Gd–Cu complex has a lower MCE with respect to the Gd-only analogue may seem surprising. The ferrimagnetism of **2** results from the antiferromagnetic $Cu^{2+}\cdots Cu^{2+}$ exchange, and it is thus clear that this type of interaction is the least favorable for observing a large MCE. Fields higher than 1–2 T are needed in order to fully break the antiferromagnetic exchanges: for $\Delta B_0 = 1$ T, $-\Delta S_m$ has a negative $-0.7\ J\,kg^{-1}\,K^{-1}$ at $T = 0.9$ K. That is, **2** acts as a cryogenic heater for this temperature and field range. This inverse behavior negatively affects the MCE of **2** for large-field changes. Complex **1** behaves likewise, although the much weaker antiferromagnetic exchange has a less pronounced effect. In contrast, the ferromagnetic exchange observed in complex **3** clearly does favor a very large MCE.

In conclusion, the complexes $[Gd^{III}_4M^{II}_8(OH)_8(L)_8(O_2CR)_8](ClO_4)_4$ are molecules in which almost all the constituent parts can be exchanged, allowing for a thorough understanding of the individual contributions to the magnetocaloric effect (MCE). In particular, the negative effect of pronounced AF exchange highlights the importance of building ferromagnetic clusters for use in low-temperature cooling.

Received: January 4, 2012
Published online: April 3, 2012

Keywords: cluster compounds · gadolinium · magnetic refrigeration · magnetocaloric effect · transition metals

[1] a) M. Evangelisti, F. Luis, L. J. de Jongh, M. Affronte, *J. Mater. Chem.* **2006**, *16*, 2534; b) M. Evangelisti, E. K. Brechin, *Dalton Trans.* **2010**, *39*, 4672.

[2] For recent examples of molecular coolers see: a) M. Evangelisti, O. Roubeau, E. Palacios, A. Camón, T. N. Hooper, E. K. Brechin, J. J. Alonso, *Angew. Chem.* **2011**, *123*, 6736; *Angew. Chem. Int. Ed.* **2011**, *50*, 6606; b) Y.-Z. Zheng, M. Evangelisti, R. E. P. Winpenny, *Angew. Chem.* **2011**, *123*, 3776; *Angew. Chem. Int. Ed.* **2011**, *50*, 3692; c) J. W. Sharples, Y.-Z. Zheng, F. Tuna, E. J. L. McInnes, D. Collison, *Chem. Commun.* **2011**, *47*, 7650; d) S. K. Langley, N. F. Chilton, B. Moubaraki, T. N. Hooper, E. K. Brechin, M. Evangelisti, K. S. Murray, *Chem. Sci.* **2011**, *2*, 1166; e) J.-B. Peng, Q.-C. Zhang, X.-J. Kong, Y.-P. Ren, L.-S. Long, R.-B. Huang, L.-S. Zheng, Z. Zheng, *Angew. Chem.* **2011**, *123*, 10837; *Angew. Chem. Int. Ed.* **2011**, *50*, 10649.

[3] See for example: a) A. Benelli, C. Benelli, A. Caneschi, R. Carlin, A. Dei, D. Gatteschi, *J. Am. Chem. Soc.* **1985**, *107*, 8128; b) M. Andruh, I. Ramade, E. Codjovi, O. Guillou, O. Kahn, J. C. Trombe, *J. Am. Chem. Soc.* **1993**, *115*, 1822; c) J. P. Costes, F. Dahan, A. Dupuis, J. P. Laurent, *Inorg. Chem.* **1997**, *36*, 3429; d) A. J. Blake, R. O. Gould, C. M. Grant, P. E. Y. Milne, S. Parsons, R. E. P. Winpenny, *J. Chem. Soc. Dalton Trans.* **1997**, 485; e) C. Benelli, D. Gateschi, *Chem. Rev.* **2002**, *102*, 2369; f) M. Evangelisti, M. L. Khan, J. Bartolomé, L. J. de Jongh, C. Meyers, J. Leandri, Y. Leroyer, C. Mathonière, *Phys. Rev. B* **2003**, *68*, 184405.

[4] Y.-Z. Zheng, M. Evangelisti, R. E. P. Winpenny, *Chem. Sci.* **2011**, *2*, 99.

[5] C. Aronica, G. Pilet, G. Chastanet, W. Wernsdorfer, J.-F. Jacquot, D. Luneau, *Angew. Chem.* **2006**, *118*, 4775; *Angew. Chem. Int. Ed.* **2006**, *45*, 4659.

[6] a) G. Karotsis, M. Evangelisti, S. J. Dalgarno, E. K. Brechin, *Angew. Chem.* **2009**, *121*, 10112; *Angew. Chem. Int. Ed.* **2009**, *48*, 9928; b) V. Mereacre, M. N. Akhtar, Y. Lan, A. M. Ako, R. Clérac, C. E. Anson, A. K. Powell, *Dalton Trans.* **2010**, *39*, 4918.

[7] S. Piligkos, Department of Chemistry, University of Copenhagen, **2010**.

[8] A. Bencini, D. Gatteschi, *Electron Paramagnetic Resonance of Exchange Coupled Systems*, Springer, Heidelberg, **1990**.

[9] W. H. Press, S. A. Teukolsky, W. T. Vetterling, B. P. Flannery, *Numerical Recipes in C: The Art of Scientific Computing*, 2nd ed., Cambridge, Cambridge University Press, **1992**.

[10] a) J. Jaklič, P. Prelovšek, *Phys. Rev. B* **1994**, *49*, 5065; b) J. Schnack, O. Wendland, *Eur. Phys. J. B* **2010**, *78*, 535.

[11] J. Schnack, P. Hage, H.-J. Schmidt, *J. Comput. Phys.* **2008**, *227*, 4512.

[12] A. J. Blake, C. M. Grant, S. Parsons, J. M. Rawson, R. E. P. Winpenny, *J. Chem. Soc. Chem. Commun.* **1994**, 2363.

